



Research Article

A Cloud-Assisted Region Monitoring Strategy of Mobile Robot in Smart Greenhouse

Xiaomin Li ¹, Zhiyu Ma ¹, Xuan Chu,¹ and Yongxin Liu²

¹College of Mechanical and Electrical Engineering, Zhongkai University of Agriculture and Engineering, Guangzhou, China

²Department of Electrical, Computer Software and Systems Engineering, Embry-Riddle Aeronautical University, Oklahoma, OK, USA

Correspondence should be addressed to Zhiyu Ma; mazhiyu2002@hotmail.com

Received 9 May 2019; Accepted 22 July 2019; Published 1 October 2019

Academic Editor: Marco Anisetti

Copyright © 2019 Xiaomin Li et al. This is an open access article distributed under the Creative Commons Attribution License, which permits unrestricted use, distribution, and reproduction in any medium, provided the original work is properly cited.

In smart agricultural systems, the macroinformation sensing by adopting a mobile robot with multiple types of sensors is a key step for sustainable development of agriculture. Also, in a region monitoring strategy that meets the real-scene requirements, optimal operation of mobile robots is necessary. In this paper, a cloud-assisted region monitoring strategy of mobile robots in a smart greenhouse is presented. First, a hybrid framework that contains a cloud, a wireless network, and mobile multisensor robots is deployed to monitor a wide-region greenhouse. Then, a novel strategy that contains two phases is designed to ensure valid region monitoring and meet the time constraints of a mobile sensing robot. In the first phase, candidate region monitoring points are selected using the improved virtual forces. In the second phase, a moving path for the mobile node is calculated based on Euclidean distance. Subsequently, the applicability of the proposed strategy is verified by the greenhouse test system. The verification results show that the proposed algorithm has better performance than the conventional methods. The results also demonstrate that, by applying the proposed algorithm, the number of monitoring points and time consumption can reduce, while the valid monitoring region area is enlarged.

1. Introduction

As it is well-known, agriculture represents the basis of many other fields. With the development of urbanization, a number of countries have faced the problem of limited farmland and urban population growth [1, 2]. The model society trends require the agriculture to improve the yield per unit of land. Therefore, precision agriculture or smart agriculture has become a hot research topic for the industry and academia as a potential solution which might solve the mentioned problem. Smart greenhouse is one of the most typical representatives of the smart agriculture that should meet the growing requirement for food. To improve the automation and efficiency of a greenhouse, the solar-powered and the water- and energy-self-sufficient method [3, 4] and the information and communication technologies

(ICTs) such as wireless sensor networks (WSNs) and intelligent control [5–8] are merged into the agricultural system. Therefore, a smart greenhouse system denotes an excellent option to realize intelligent and precision agriculture.

The data collection, especially macrodata collection, represents a precondition for the realization of a smart greenhouse. With the development of information collection technologies [9–11], the ICTs have been gradually introduced in a greenhouse, and the agricultural WSNs have become classical applications for information gathering. The agricultural WSNs have obtained a great progress [12–14]. However, on the one hand, current WSNs are mostly composed of static nodes and constraint of energy charging, so that the monitoring systems lack the flexibility and lifespan [15]. On the other hand, with the increase in greenhouse size, the monitoring region is becoming wider

[16]. Accordingly, traditional WSNs are not suitable for greenhouse region monitoring.

Many studies have been devoted to solving the data collection in greenhouse; namely, more and more WSN nodes have been deployed to meet the trends but that has increased the system cost significantly, especially for a large-region greenhouse [17, 18]. Besides, many studies have been focused on reducing energy consumption, but all proposed methods still have a constraint of limited energy of WSNs [19, 20]. Accordingly, to increase the mobility and flexibility simultaneously, mobile elements (a mobile robot or a mobile sensor node) have been introduced to the system. The related studies have also researched on this topic from different perspectives such as path planning and obstacle avoidance [21–23]. However, the greenhouse region monitoring still faces the following problems: (1) how to construct a more efficient framework using the cloud computing and mobile elements to improve the data collection and (2) how to choose a better moving path for the greenhouse region monitoring with latency and energy constraints.

Recently, the cyber-physical system (CPS) has been more and more introduced into the agriculture. Motivated by the advantages of the CPS, especially cloud technologies, and the features of greenhouse region monitoring, we present a novel solution to solve these mentioned problems.

The contributions of this work can be summarized as follows:

- (1) A novel data collection system based on cloud computing, wireless networks, and mobile nodes is developed
- (2) To meet the requirements for region monitoring ratio and time consumption, a cloud-assisted region monitoring strategy of mobile robot is designed
- (3) To evaluate the framework and strategy, a real experiment is conducted, and the obtained results are discussed

The remainder of this paper is organized as follows: Section 2 introduces related work about information collection and region monitoring in agriculture. Section 3 gives the cloud-assisted information collection frameworks for smart greenhouse. Section 4 proposes the method information collection. Section 5 evaluates the proposed algorithm experimentally and discusses the obtained results. Section 6 concludes the paper.

2. Related Work

2.1. Information Collection in Agriculture. As it is well-known, data collection represents the basis of smart greenhouse. Therefore, numerous studies have been focused on the data collection method. In [24], to achieve scientific cultivation and reduce management costs, a wireless sensor network architecture was adopted in the vegetable greenhouse to monitor environmental parameters. In [25], to schedule irrigation, the authors proposed a multiple sensor system to collect soil moisture and weather parameters. Then, using the collected data, the equipment was driven for

precision irrigation. In [26], a wireless sensor network was adopted to detect the presence of snails by sensing the environmental data. The WSN nodes were also designed with real application and deployed in the data collection. As the climate is a significant factor for crop yield and diseases, in [27], the authors realized a distributed monitoring system for a greenhouse using a WSN and analyzed the raw data to explore the condition of growing crops. In [28], the authors designed a farmland information collection system containing a portable farmland information collection device, a remote server, and a mobile phone APP. Furthermore, this system was implemented, and the information about collected air temperature and humidity, chlorophyll, and other farmland-related information was collected. In [29], by equipping wireless sensors on tractors and other equipment, a delay disruption tolerant information collection system was designed and implemented in the farmland. Different information collection method and applications were proposed in the aforementioned studies. However, the proposed solutions are mostly based on static wireless sensor networks and are not suitable for region monitoring in a smart greenhouse.

2.2. Region Monitoring Methods. With the development of information analysis, many studies demonstrated that region monitoring could be adopted to monitor the objective targets [30, 31]. In some studies, the increasing number of mobile nodes was used for region monitoring. In [32], the authors presented a distributed framework containing a server and clients running different strategies to monitor the region, which was impossible to install fixed cameras, based on the crowdsourcing and mobile device. In [33], mobile nodes in the wireless sensor network were used to monitor the uncovered region. Then, an algorithm was used to find out an optimal path of a mobile node to cover the target region. Recently, drones which are the type of unmanned aerial vehicles (UAVs) have made progress in the field, thus providing a good solution for the region monitoring problem. In [34], a UAV was used as a mobile information collector for region monitoring. Also, the region to be monitored was divided into cells. The author assigned to each UAV the cells to visit and optimized the path of each UAV by considering fairness. In addition, in [35], the authors used drones to monitor large regions effectively. Also, by combining the skyline query, a new strategy was proposed to search a more suitable UAV flying path. The abovementioned studies provide a reference and new solutions for the greenhouse region monitoring problem. However, to meet region monitoring, the greenhouse characteristics and low latency of region monitoring need to be considered.

3. Cloud-Assisted Data Collection Framework for Smart Greenhouse

In the section, a region monitoring architecture in a greenhouse is presented, the working process of the

framework is explained, and the mobile robot is introduced.

3.1. Information Collection Framework for Greenhouse. With the development of Internet of Things (IoT) and cloud computing technologies, the ICTs have been proved as effective methods for information collection. Since the traditional frameworks for greenhouse lack the mobility, computing resources, and collection, the previous solutions are not gradually suitable for the new requirement. To improve the flexibility and scalability of a smart greenhouse, the wireless network, cloud computing, software applications, and greenhouse equipment are merged into an improved framework. The proposed framework for smart system sensing consists of three layers: the network layer, the cloud layer, and the application layer and the data sensing field, as shown in Figure 1. Meanwhile, all the components are linked by either wired or wireless networks and internet of things (IoT). We solely agree that big data analysis and artificial intelligence are the future trend in agriculture. The distributed cloud services, as far as we can see, are the most flexible and cost-efficient infrastructure for big data analysis in smart agriculture. It is known that cloud has become an important part for the smart agriculture. On the one hand, the proposed algorithm easily gets the global information for achieving the optimal results by using cloud technologies. On the other hand, big data is not in conflict with the cloud, as cloud is the basic platform of big data analysis.

In the application layer, different applications are constructed to meet the real requirements such as that for greenhouse management, data visualization, and mobile terminal operations. Data storage and computing task are performed in the cloud layer. In network layers, the data transfer is conducted via either wired or wireless networks. Meanwhile, the data sensing field is used to collect data from different sensors of greenhouse such as temperature, humidity, light level, image of crop, and other parameters.

3.2. Mobile Region Monitoring Robot in the Framework. In the paper, the focus is on region monitoring in a greenhouse using a mobile robot. Therefore, a brief review of a mobile region-monitoring robot (MAMR) is provided. A MAMR is equipped with a wireless radio module, a power unit, and different sensors such camera and humiture sensor. The application layer or cloud servers conduct the region monitoring task; namely, the cloud server decomposes the task into multiple steps and determines the key orders to the mobile nodes according to the greenhouse global information. Then, the MAMR finishes the region monitoring following the cloud issuing orders. Finally, when a mobile node moves along the planning path, it transmits the information to the cloud server through the IoT system.

4. Mobile Robot Region Monitoring Strategy in Greenhouse

In the section, we first provide the problem formulation. Then, we present a region monitoring strategy for mobile robots, which contains two phases: candidate point selecting and moving path searching.

4.1. Problem Formulation. For the sake of simplicity, we consider a greenhouse as a flat rectangular and let $\Lambda \subset R^2$ be a flat rectangular region of a greenhouse. Also, we assume that, in a certain time period, there are n regions to be monitored and let $\Delta = \{\delta_1, \delta_2, \dots, \delta_n\}$ ($\delta_i \subset \Delta$, $\Delta \subset \Lambda$) be the set of these regions. Meanwhile, we assume that each monitoring region δ_i has a trajectory and starting point $x_0(\delta_i)$. A mobile robot equipped with different sensors is navigated through the defined monitoring region along the trajectory. Assume that a MAMR monitors region δ_i at certain points, which are on a trajectory tr_{δ_i} . There are $m(\delta_i)$ monitoring points on the trajectory tr_{δ_i} . Let R be the sensing radius. In this work, a MAMR monitoring region is denoted as a circle. The set of monitoring circles is expressed as $C(\delta_i) = \{c_1, c_2, \dots, c_{m(\delta_i)}\}$ and the set of circles' center locations is expressed as $X(\delta_i) = \{x_1(\delta_i), x_2(\delta_i), \dots, x_{m(\delta_i)}(\delta_i)\}$, and it is arranged according to the distance from the starting point of a monitoring region δ_i .

Definition 1. Real monitoring area (RMA): let $c_k(\delta_i)$ be a monitoring region, where $k \in m(\delta_i)$. The real monitoring area $\alpha(\delta_i)$ of δ_i can be defined as follows:

$$\alpha(\delta_i) = S\left[\left(c_1 \cup c_2 \cup \dots \cup c_{m(\delta_i)}\right) \cap \delta_i\right], \quad (1)$$

where $S[\cdot]$ denotes the function for getting a real monitoring area of a mobile robot. Let $c_k \cap \delta_i$ be a valid monitoring region of monitoring circle and monitoring region δ_i . Thus, (1) can be simplified as follows:

$$\alpha(\delta_i) = S\left[\bigcup_{k \in m(\delta_i)} (c_k \cap \delta_i)\right]. \quad (2)$$

Furthermore, let $T_s(x_k(\delta_i))$ be the sensing time of a MAMR at the point $x_k(\delta_i)$ of the monitoring region δ_i . Thus, $T_s(X(\delta_i))$ denotes the total sensing time of δ_i , and it is given by

$$T_s(X(\delta_i)) = \sum_{k \in m(\delta_i)} T_s(x_k(\delta_i)). \quad (3)$$

Assume that sensing time at any point is constant τ , so (3) can be simplified as

$$T_s(X(\delta_i)) = m(\delta_i) \cdot \tau. \quad (4)$$

Therefore, the total sensing time of Δ $T_s(\Delta)$ is given by

$$\begin{aligned} T_s(\Delta) &= (m(\delta_1) + m(\delta_2) + \dots + m(\delta_n))\tau \\ &= \tau \sum_{i \in n} m(\delta_i). \end{aligned} \quad (5)$$

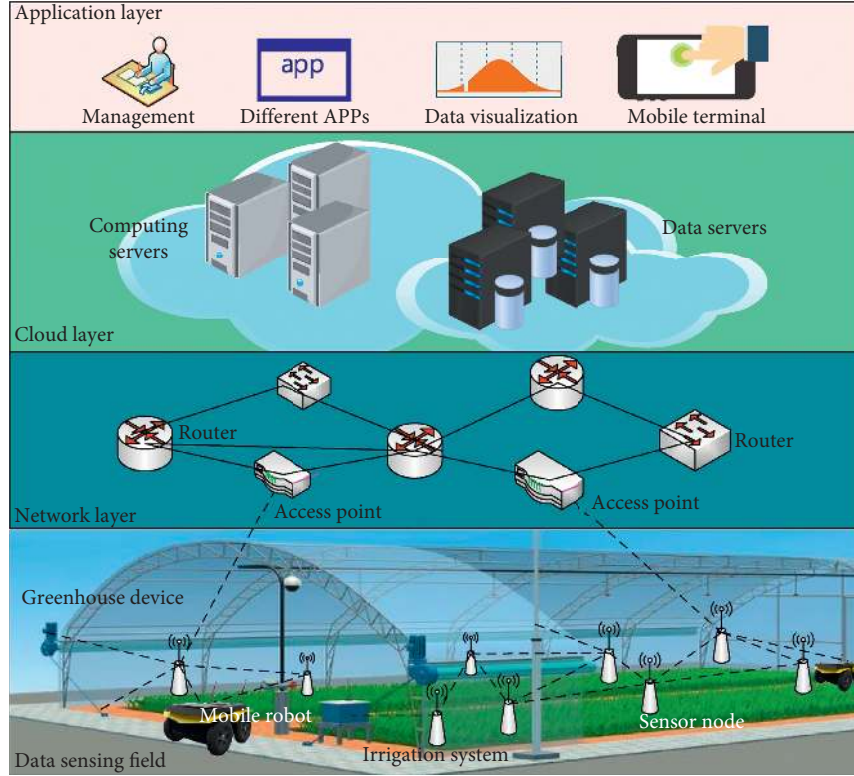


FIGURE 1: Information collection architecture for greenhouse.

According to the above relations, let $T(\delta_i)$ be the time consumption, which includes the moving time and monitoring time $T_{\text{move}}(X(\delta_i))$ of a monitoring region δ_i , and it is expressed as

$$T(\delta_i) = \tau \cdot m(\delta_i) + T_{\text{move_point}}(X(\delta_i)). \quad (6)$$

Moreover, let $T_{\text{move_region}}(\Delta)$ be the moving time through a monitoring region. In summary, the total time consumption of all the monitoring regions can be calculated as

$$\begin{aligned} T &= T_{\text{move_region}}(\Delta) + \sum_{i \in n} T(\delta_i) \\ &= T_{\text{move_region}}(\Delta) + \tau \sum_{i \in n} m(\delta_i) + \sum_{i \in n} T_{\text{move_point}}(X(\delta_i)). \end{aligned} \quad (7)$$

Definition 2. Region monitoring ratio (RMR): let $\alpha(\delta_i)$ and $\gamma(\delta_i)$ be the real area of monitoring and the area of δ_i , respectively. The region monitoring rate of a monitoring region δ_i , denoted as $\varepsilon(\delta_i)$, is a fraction of the real monitoring area within the area of δ_i , and it can be expressed as

$$\varepsilon(\delta_i) = \frac{\alpha(\delta_i)}{\gamma(\delta_i)}. \quad (8)$$

Therefore, the region monitoring ratio of a whole greenhouse can be expressed as

$$E(\Delta) = \frac{\sum_i \alpha(\delta_i)}{\sum_i \gamma(\delta_i)}. \quad (9)$$

Assume that there is a constant area in each δ_i , and then (9) can be approximated as

$$E(\Delta) = \frac{\sum_i \alpha(\delta_i)}{n \cdot \gamma(\delta_i)} = \frac{1}{n} \sum_{i \in n} \frac{\alpha(\delta_i)}{\gamma(\delta_i)} = \frac{1}{n} \sum_{i \in n} \varepsilon(\delta_i). \quad (10)$$

Definition 3. Covering path (CP): CP is the moving path of a MAMR that covers all the monitoring regions. Let P be the CP set, which can be formulated as

$$P = \{p_i \mid p_i \Upsilon \Delta\}, \quad (11)$$

where $p_i \Upsilon \Delta$ denotes that p_i covers all the regions.

Each monitoring area tries to get its RMR that should be larger than the preset constant. Thus, the objective of this paper is to search a path from P to meet the above requirement of RMR while meeting the following requirements:

$$\begin{aligned} E(\Delta) &\geq \bar{E}, \\ T &\leq T_{\text{deadline}}, \\ 0 &< \varepsilon(\delta_i) \leq 1, \end{aligned} \quad (12)$$

where $\bar{E} = \{\varepsilon_1, \varepsilon_2, \dots, \varepsilon_n\}$ is the preset value of the RMR and T_{deadline} is the deadline of the monitoring region.

4.2. Proposed Method for Mobile Robot-Based Region Monitoring. Solving the problem defined by (12) is challenging due to the following reasons. The time consumption is related to the number of monitoring points and path length. In this section, we divide the problem (12) into two subproblems: selecting candidate monitoring points and an optimal region monitoring moving path. First, an improved virtual force is employed for selecting candidate points. Then, to meet the monitoring time consumption requirement, we develop an algorithm based on simulated annealing for determining an optimal moving path.

4.2.1. Selecting Strategy for Candidate Monitoring Points.

In the traditional virtual force model, the force directions are random. It is known that the model is not suitable for a greenhouse. Meanwhile, the monitoring points are on the monitoring trajectory. Accordingly, we use a single direction along with the trajectory.

Meanwhile, a coverage coefficient $\beta(\delta_i)$ of a monitoring region δ_i is introduced to the model, and it is formulated as

$$\beta(\delta_i) = \begin{cases} 1, & \varepsilon(\delta_i) \geq \varepsilon_i, \\ 0, & \text{otherwise.} \end{cases} \quad (13)$$

Thus, according to Hooke's law, the virtual force is formulated as

$$f_{pq} = \begin{cases} \beta(\delta_i)k \cdot |d|, & d_{lq} \leq 2R, \\ -\beta(\delta_i)k \cdot |d|, & d_{lq} > 2R, \end{cases} \quad (14)$$

where k denotes the virtual force coefficient and $|d| = |2R - d_{lp}|$. So, the total virtual force between the monitoring points (l, q) can be expressed as

$$\overrightarrow{F_q(\delta_i)} = \sum_{l \in P} \overrightarrow{f_{lq}}. \quad (15)$$

Furthermore, the total virtual force of monitoring point set P can be formulated as

$$\overrightarrow{F(\delta_i)} = \frac{1}{2} \sum_{Q \in P} \overrightarrow{F_q(\delta_i)}. \quad (16)$$

According to the above relations, we minimize the virtual force to determine the minimal number of monitoring points:

$$\begin{aligned} \text{Min} \quad & \left(\overrightarrow{F(\delta_i)} \right) \\ \text{subject to} \quad & p \in \delta_i \\ & \varepsilon(\delta_i) \geq \varepsilon_i. \end{aligned} \quad (17)$$

To solve the problem given by (17), we use the following equations to update a new location $X_q(\text{next})$ according to the current position $X_q(\text{current})$:

$$X_q(\text{next}) = \begin{cases} X_q(\text{next}), & |F| \leq F_{\text{TH}}, \\ X_q(\text{next}) + d_{\text{move}} \cdot e^{(-1/F)}, & |F| > F_{\text{TH}}, \end{cases} \quad (18)$$

where d_{move} is the moving distance of each iteration and F_{TH} is the threshold value of virtual force. The proposed strategy for selecting strategy for candidate monitoring points is shown in Algorithm 1, and it can be explained as follows: first, in the initialization step, the preset values of the variables are set. Then, the virtual force is calculated according to the corresponding equations. If the virtual force is larger than the threshold value, a new location of monitoring points is updated, and if the virtual force is less than the threshold value, the monitoring location would stop updating. Also, the RMR is calculated and judged whether its value meets the requirement. The iteration steps repeat until all the constraints are met.

4.2.2. Hybrid Solution for Optimal Moving Path. To obtain the shortest moving path, we divide the strategies of searching the optimal moving path into two stages: intermonitoring region and outermonitoring region. In the first stage, a greedy strategy is used to get the shortest moving path. In the second stage, the problem is first classified as a traveling salesman problem (TSP), and then a simulated annealing is used to solve it.

4.2.3. Stage I: Intermonitoring Region. After Algorithm 1 is finished, in the monitoring region δ_i , the number of monitoring points and their locations can be obtained. The moving path of a mobile robot must contain the stating points, so the extended monitoring point set is defined as follows:

$$P^+(\delta_i) = P(\delta_i) \cup O(\delta_i), \quad (19)$$

where $O(\delta_i)$ denotes the starting point of a trajectory tr_{δ_i} . Furthermore, the location set that corresponds to the extended monitoring point set can be expressed as

$$X^+(\delta_i) = \left\{ 0, x_1(\delta_i), x_2(\delta_i), \dots, x_{m(\delta_i)}(\delta_i) \right\}, \quad (20)$$

where 0 denotes the location of $O(\delta_i)$. Let $\text{NBP}_p(\delta_i)$ be the neighboring point of p . Then, the Euclidean distance between p and any of its neighboring point q can be expressed as

$$d_{pq} = \sqrt{(x_p - x_q)^2} \quad (q \in \text{NBP}_p(\delta_i)). \quad (21)$$

As all the monitoring points are on the trajectory, to get an optimal moving path within the monitoring region, a greedy strategy is designed based on the neighboring distance; namely, in each iteration, the nearest neighboring point is selected as the next moving point. The process steps are given in Algorithm 2. First, using (19) and (20), the extended monitoring point set and the corresponding location set are determined, respectively. Next, the neighboring point set is created based on the distance value. Then, the neighboring point at the minimal distance is selected as the next moving point. Finally, the algorithm returns the moving path points and their locations of the monitoring region.

```

Input:  $\varepsilon_i, R, F_{TH}, max\_iteration, d_{moving}$ 
Output:  $m(\delta_i), X(\delta_i)$ 
Initialize  $m(\delta_i) = 1, X(\delta_i) = R$ 
repeat
  while  $(h < max\_interaction)$ 
    if  $\overrightarrow{F(\delta_i)}(h) \geq \overrightarrow{F(\delta_i)}(h-1)$ 
      for  $l : m(\delta_i)$ 
        Calculate virtual force  $\overrightarrow{F(\delta_i)}$ 
        if  $|\overrightarrow{F(\delta_i)}| \leq F_{TH}$ 
          update location according to (18)
          if  $X_q(next) \in \delta_i$ 
             $X_q(next) \leftarrow X_q(next)$ 
          else
             $X_q(next) \leftarrow X(\text{boundary})$ 
          calculate the total force
         $m(\delta_i) \leftarrow m(\delta_i) + 1$ 
      until  $\varepsilon(\delta_i) \geq \varepsilon_i$ 
Return  $m(\delta_i), X(\delta_i)$ 

```

ALGORITHM 1: Selecting candidate monitoring points based on improved virtual force.

```

Input:  $P(\delta_i), X(\delta_i) = \{x_1(\delta_i), x_2(\delta_i), \dots, x_{m(\delta_i)}(\delta_i)\}$ 
Output:  $P_{move}(\delta_i)$ 
Initialization:  $MP(\delta_i) = \{O\}$ 
 $P^+(\delta_i) \leftarrow P(\delta_i) \cup O(\delta_i)$ 
 $X^+(\delta_i) \leftarrow \{0, x_1(\delta_i), x_2(\delta_i), \dots, x_{m(\delta_i)}(\delta_i)\}$ 
for  $f:1:|P^+(\delta_i)|$ 
  Search neighboring points of  $p_f^+(\delta_i)$ 
  Create neighboring points set  $NBP_f(\delta_i)$ 
  for  $q:1:NBP_f(\delta_i)$ 
    Calculate the distance according (21)
  Creating distance set of all neighboring points
  Selecting the minimal distance point  $P_{min}^f$ 
   $MP(\delta_i) = MP(\delta_i) + P_{min}^f$ 
   $NBP_{P_{min}^f}(\delta_i) - P_f(\delta_i)$ 
return  $MP(\delta_i)$ 

```

ALGORITHM 2: Moving path in the intermonitoring region.

4.2.4. *Stage II: Outer Monitoring Region.* In stage I, the moving path in the intermonitoring region is solved. Next, in the second stage, we focus on obtaining the shortest moving path in the outer monitoring region.

In the previous stage, the monitoring points in each monitoring subregion are obtained. Since the monitoring points' distances are smaller than the distance between the subregions, the barycenter method is used for monitoring points' locations normalization. Specifically, in a subregion δ_i , the barycenter can be formulated as

$$\overline{X(\delta_i)} = \frac{\sum_{q \in P(\delta_i)} x_p}{|P(\delta_i)|}. \quad (22)$$

So, the barycenter of all the subregions can be expressed as

$$\overline{X} = \{\overline{X(\delta_1)}, \overline{X(\delta_2)}, \dots, \overline{X(\delta_n)}\}. \quad (23)$$

With regard to the above discussion, the outer shortest moving path selection can be transferred into a TSP problem. To solve the TSP problem, the simulated annealing is employed. The process of determining an optimal moving path in the outer monitoring region is given in Algorithm 3. In Algorithm 3, first the barycenter of each subregion is calculated; then, simulated annealing is used to obtain the shortest moving path, and finally, the algorithm returns the results to the mobile robot.

5. Experimental Results

The proposed algorithm was evaluated experimentally. The obtained experimental results are presented and discussed in terms of different metrics. Besides, the proposed algorithm is compared with the traditional methods regarding the following three aspects: the number of monitoring points, average covering area, and time consumption.

```

Input:  $P(\delta_i)$ ,  $X(\delta_i) = \{x_1(\delta_i), x_2(\delta_i), \dots, x_{m(\delta_i)}(\delta_i)\}$ 
Output:  $P_{\text{move}}(\Delta)$ 
Initialization:  $P_{\text{move}}(\Delta) = \emptyset$ ,  $\bar{X} = \emptyset$ .
for  $i:1:n$ 
     $\bar{X}(\delta_i) \leftarrow \sum_{q \in P(\delta_i)} x_p / |P(\delta_i)|$ 

     $\bar{X} \leftarrow \bar{X} + \bar{X}(\delta_i)$ 
    SA initialization//simulated annealing
Repeat
    Metropolis sampling algorithm
    Calculate the corresponding target function value
until
    The current solution  $X_{\text{move}}$  is an optimal solution
Return  $X_{\text{move}}$ 

```

ALGORITHM 3: Moving path in the outer monitoring region.

5.1. Experimental Settings. A real experiment was performed using a mobile robot in the greenhouse that was planted with different crops, as shown in Figure 2. A hybrid method that contains the ultrasonic obstacle avoidance and automatic tracking (different colors) is adopted to cope with the robot obstacle avoidance. The mobile robot was equipped with many sensors to collect air temperature, humidity, and light intensity and a camera.

In order to demonstrate that the proposed planning algorithm performs correctly in a real environment, an experimental setup presented in Figure 2 was constructed. The experimental settings were as follows. The greenhouse area was $\Lambda = 40 \times 50 \text{ m}^2$, and it contained 10 subregions with the same size of $2 \times 4 \text{ m}^2$. The sensing radius R was 1 m. The other experimental parameters are given in Table 1. The proposed strategy was applied for several times, and the average results were calculated.

As already mentioned, there are few works that address the region monitoring problem. Therefore, we compared our method called the CARM with the following common methods: (1) the SSRL method which selects the same number of the monitoring points in a subregion as the CARM, but with a with random location; (2) the FMPS method which selects fixed monitoring location at the same distance along the trajectory. In the experiments, the distance of points was equal to the sensing radius.

5.2. Result Analysis

5.2.1. Number of Monitoring Points. The average number of monitoring points of different methods corresponding to their best performances in the real experiment is presented in Figure 3(a); namely, the average number of monitoring points at the RMR of 20%, 70%, and 90% of different methods is presented in Figure 3(a). In Figure 3(a), it can be seen that the average number of monitoring points increased with the increase in the RMR for all the methods. However, the CAMR outperformed the other methods in all the three cases, which was due to the optimization virtual force algorithm of the CAMR method which selected a more optimal number of monitoring

points and their locations. The FMPS achieved better performance than the SSRL because monitoring points were evenly distributed along the trajectory. At the RMR of 70%, the CARM had almost 20% and 10% smaller average number of monitoring points than the SSRL and the FMPS, respectively.

5.2.2. Average Coverage Area. The average coverage area of different methods is presented in Figure 3(b). In Figure 3(b), it can be seen that, for all the values of the number of monitoring points, the average coverage area of the proposed method was the best because the CARM selected the most optimal number of monitoring points and their locations in order to get a large coverage area. As displayed in Figure 3(b), the SSRL obtained poor average coverage area performance because of random monitoring points selection which was employed in this method. Moreover, by increasing the number of monitoring points, the average coverage area performance enhanced for all the methods. In addition, when the number of points was 3, the coverage area of the CARM was larger than 35 m^2 . Besides, the CARM could adapt to a different number of monitoring points and had the best average coverage area performance among all the tested methods.

5.2.3. Time Consumption. The total sensing time consumption performance for each subregion of different methods at the RMR of 70% is presented in Figure 4(a). In general, the total sensing time of each method increased with the increase in the sensing time of a single point. The CARM achieved the best performance regarding this metric; in other words, the CARM took less time to finish the monitoring task than the other two methods. When the RMR was 70% and the sensing time of a single point was 5 s, the total sensing time consumption of the CARM was less than 15 s, while the other methods had longer sensing time, especially the SSRL because this method selected more points for monitoring.

The total time consumption performance at a different moving speed for the whole monitoring region of different



FIGURE 2: The experimental scene.

TABLE 1: Experimental parameter.

Parameter	Value
Virtual force threshold	0
Number of monitoring subregions	5
Sensing radius	1 m
Sensing time of a single point	0.5~5 s
Robot moving speed	0.05~0.5 m/s
Deadline of the monitoring region	100~500 s
Region monitoring ratio	40~50%
Length of subregion trajectory	200 m

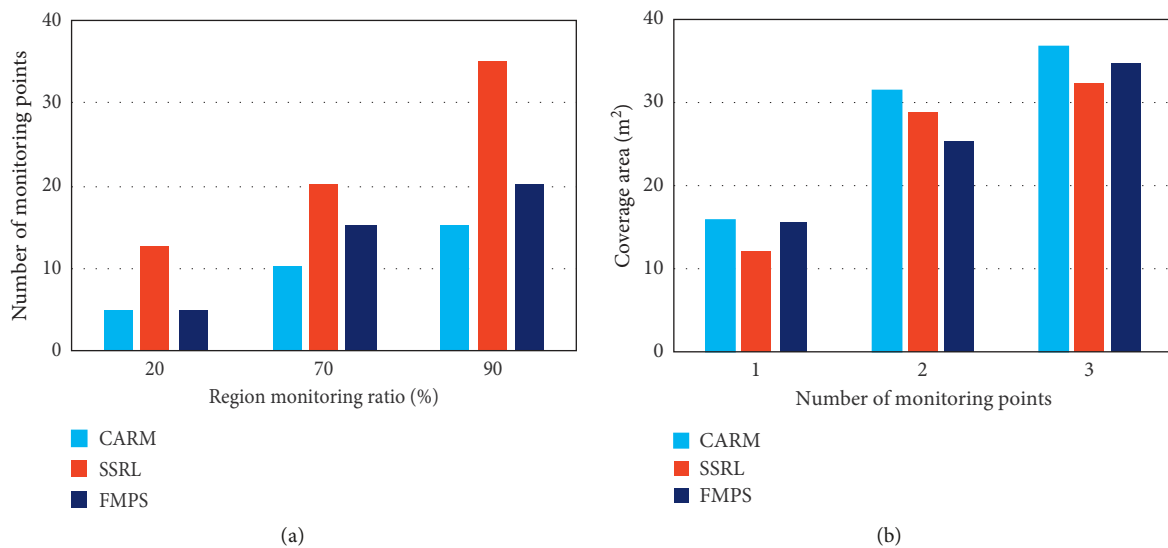


FIGURE 3: (a) Number of monitoring points and (b) coverage area of different methods.

methods at the RMR of 70% is presented in Figure 4(b). Generally, as the robot moving speed increased, the total time consumption reduced. Therefore, the total time consumption of all the methods decreased with the increase in the robot moving speed. Similarly, the CARM achieved the best performance in terms of the total time consumption which means that the CARM finished the monitoring task faster than the other methods, which was because the optimal algorithm was used to select the number of monitoring points and their locations. Meanwhile, at the RMR of 70%,

the robot moving speed of 0.5 m/s, and the sensing time of a single point of 5 s, the CARM had 5% and 3% shorter total sensing time consumption compared to the SSRL and FMPS methods, respectively.

5.2.4. Cost Evaluation. It is known that cost evaluation is an essential part of the practical application. Obviously, according to Figures 3 and 4, the proposal method CARM can reduce the number of monitoring points for the same

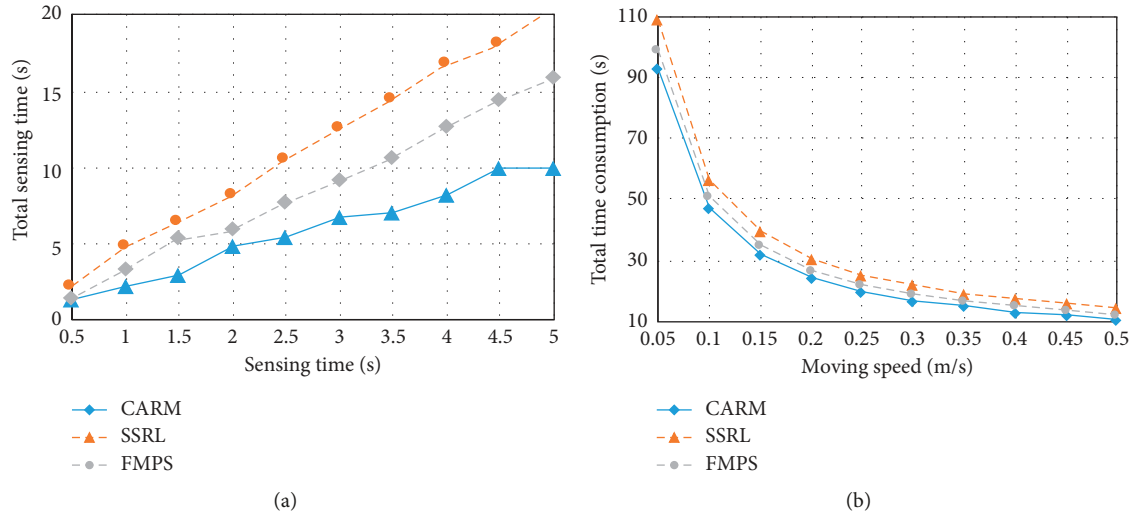


FIGURE 4: Time consumption of different methods: (a) total sensing time; (b) total time consumption.

coverage area and decrease the time consumption comparing the traditional methods SSRL and FMPS. In other words, the proposed strategy can get lower maintenance cost. Indeed, the presented framework because of needing to build a cloud is more expensive than the traditional region monitoring framework, such as WSN. However, the public clouds can significantly reduce costs, as public clouds present a very low price (0.023~0.04 dollar/GB for data storage and 0.017~0.027 dollar/GB RAM of Amazon Web Services); furthermore, some companies offer free cloud services. Besides, private farms in China could not afford to hire professional technicians for maintenance of private servers, so, compared with using dedicated servers, making use of the public cloud is the most feasible solution.

6. Conclusions

An efficient region monitoring of plants in a smart greenhouse is important but challenging. In this paper, we propose a novel cloud-assisted region monitoring strategy of mobile robots based for a smart greenhouse to increase the monitoring region size and reduce the time consumption. First, an information collection framework based on mobile robots, wireless network, and cloud computing is introduced. Then, the region monitoring model of a mobile robot with cloud computing is constructed in accordance with the greenhouse features and cloud resources. Moreover, based on the model, two strategies are proposed to select the candidate monitoring points by adopting the improved virtual force and a hybrid solution for the optimal moving path. The proposed algorithm is verified by real experiments in the greenhouse. The experimental results demonstrate that the proposed algorithm can provide more efficient region monitoring of greenhouse than the conventional methods.

Data Availability

The data used to support the findings of this study are available from the corresponding author upon request.

Conflicts of Interest

The authors declare there are no conflicts of interest regarding the publication of this paper.

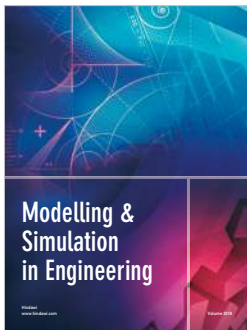
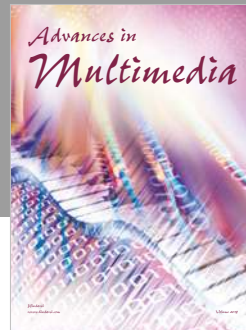
Acknowledgments

This paper was supported by the Science and Technology Planning Project of Guangdong Province, China (no. 2014A020208132), and Science and Technology Project of Guangzhou, China (no. 201607010018).

References

- [1] K. L. Skog and M. Steinnes, "How do centrality, population growth and urban sprawl impact farmland conversion in Norway?," *Land Use Policy*, vol. 59, pp. 185–196, 2016.
- [2] W. Song, B. C. Pijanowski, and A. Tayyebi, "Urban expansion and its consumption of high-quality farmland in Beijing, China," *Ecological Indicators*, vol. 54, no. 54, pp. 60–70, 2015.
- [3] E. Farrell, M. I. Hassan, R. A. Tufa et al., "Reverse electro-dialysis powered greenhouse concept for water- and energy-self-sufficient agriculture," *Applied Energy*, vol. 187, pp. 390–409, 2017.
- [4] S. Suryawanshi, S. Ramasamy, S. Umashankar, and P. Sanjeevikumar, "Design and implementation of solar-powered low-cost model for greenhouse system," in *Advances in Smart Grid and Renewable Energy*, vol. 435, pp. 357–365, Springer, Berlin, Germany, 2018.
- [5] G. Ping, P. Dusadeeringsikul, and S. Y. Nof, "Agricultural cyber physical system collaboration for greenhouse stress management," *Computers & Electronics in Agriculture*, vol. 150, pp. 439–454, 2018.
- [6] X. Bai, Z. Wang, L. Sheng, and Z. Wang, "Reliable data fusion of hierarchical wireless sensor networks with asynchronous measurement for greenhouse monitoring," *IEEE Transactions on Control Systems Technology*, vol. 27, no. 3, pp. 1036–1046, 2018.
- [7] P. J. Kia, A. T. Far, M. Omid, R. Alimardani, and L. Naderloo, "Intelligent control based fuzzy logic for automation of greenhouse irrigation system and evaluation in relation to

- conventional systems,” *World Applied Sciences Journal*, vol. 6, no. 1, pp. 16–23, 2009.
- [8] A. Somov, D. Shadrin, I. Fastovets et al., “Pervasive agriculture: IoT-enabled greenhouse for plant growth control,” *IEEE Pervasive Computing*, vol. 17, no. 4, pp. 65–75, 2018.
- [9] X. Li, D. Li, J. Wan, C. Liu, and M. Imran, “Adaptive transmission optimization in SDN-based industrial internet of things with edge computing,” *IEEE Internet of Things Journal*, vol. 5, no. 3, pp. 1351–1360, 2018.
- [10] J. Wan, J. Li, Q. Hua, A. Celesti, and Z. Wang, “Intelligent equipment design assisted by cognitive internet of things and industrial big data,” *Neural Computing and Applications*, pp. 1–10, 2018.
- [11] J. Wan, J. Li, M. Imran, and D. Li, “A blockchain-based solution for enhancing security and privacy in smart factory,” *IEEE Transactions on Industrial Informatics*, vol. 15, no. 6, pp. 3652–3660, 2019.
- [12] L. D. Pedrosa, P. Melo, R. M. Rocha, and R. Neves, “A flexible approach to WSN development and deployment,” *International Journal of Sensor Networks*, vol. 6, no. 3/4, pp. 199–211, 2009.
- [13] X.-M. Guo, X.-T. Yang, M.-X. Chen, M. Li, and Y.-A. Wang, “A model with leaf area index and apple size parameters for 2.4 GHz radio propagation in apple orchards,” *Precision Agriculture*, vol. 16, no. 2, pp. 180–200, 2015.
- [14] D. Upadhyay, A. K. Dubey, and P. S. Thilagam, “Application of non-linear Gaussian regression-based adaptive clock synchronization technique for wireless sensor network in agriculture,” *IEEE Sensors Journal*, vol. 18, no. 10, pp. 4328–4335, 2018.
- [15] O. Elijah, T. A. Rahman, I. Orikumhi, C. Y. Leow, and M. N. Hindia, “An overview of internet of things (IoT) and data analytics in agriculture: benefits and challenges,” *IEEE Internet of Things Journal*, vol. 5, no. 5, pp. 3758–3773, 2018.
- [16] M. Kang, X.-R. Fan, J. Hua, H. Wang, X. Wang, and F.-Y. Wang, “Managing traditional solar greenhouse with cpsps: a just-for-fit philosophy,” *IEEE Transactions on Cybernetics*, vol. 48, no. 12, pp. 3371–3380, 2018.
- [17] X. Bai, Z. Wang, L. Zou, and F. E. Alsaadi, “Collaborative fusion estimation over wireless sensor networks for monitoring CO₂ concentration in a greenhouse,” *Information Fusion*, vol. 42, pp. 119–126, 2018.
- [18] D.-H. Park, B.-J. Kang, K.-R. Cho et al., “A study on greenhouse automatic control system based on wireless sensor network,” *Wireless Personal Communications*, vol. 56, no. 1, pp. 117–130, 2011.
- [19] Y. Zhang, H. Gao, S. Cheng, and J. Li, “An efficient EH-WSN energy management mechanism,” *Tsinghua Science and Technology*, vol. 23, no. 4, pp. 406–418, 2018.
- [20] W. Xu, Y. Zhang, Q. Shi, and X. Wang, “Energy management and cross layer optimization for wireless sensor network powered by heterogeneous energy sources,” *IEEE Transactions on Wireless Communications*, vol. 14, no. 5, pp. 2814–2826, 2015.
- [21] C.-H. Ou and W.-L. He, “Path planning algorithm for mobile anchor-based localization in wireless sensor networks,” *IEEE Sensors Journal*, vol. 13, no. 2, pp. 466–475, 2013.
- [22] A. Alomari, W. Phillips, N. Aslam, and F. Comeau, “Swarm intelligence optimization techniques for obstacle-avoidance mobility-assisted localization in wireless sensor networks,” *IEEE Access*, vol. 6, pp. 22368–22385, 2018.
- [23] P. Zhou, C. Wang, and Y. Yang, “Static and mobile target k-coverage in wireless rechargeable sensor networks,” *IEEE Transactions on Mobile Computing*, vol. 18, no. 10, pp. 2430–2445, 2019.
- [24] M. Srbinovska, C. Gavrovski, V. Dimcev, A. Krkoleva, and V. Borozan, “Environmental parameters monitoring in precision agriculture using wireless sensor networks,” *Journal of Cleaner Production*, vol. 88, pp. 297–307, 2015.
- [25] R. Sui and J. Baggard, “Wireless sensor network for monitoring soil moisture and weather conditions,” *Applied Engineering in Agriculture*, vol. 31, no. 2, pp. 193–200, 2015.
- [26] D. Garcia-Lesta, D. Cabello, E. Ferro, P. Lopez, and V. M. Brea, “Wireless sensor network with perpetual motes for terrestrial snail activity monitoring,” *IEEE Sensors Journal*, vol. 17, no. 15, pp. 5008–5015, 2017.
- [27] K. P. Ferentinos, N. Katsoulas, A. Tzounis, T. Bartzanas, and C. Kittas, “Wireless sensor networks for greenhouse climate and plant condition assessment,” *Biosystems Engineering*, vol. 153, pp. 70–81, 2017.
- [28] J. Zhang, J. Hu, L. Huang, Z. Zhang, and Y. Ma, “A portable farmland information collection system with multiple sensors,” *Sensors*, vol. 16, no. 10, Article ID 1762, 2016.
- [29] H. Ochiai, H. Ishizuka, Y. Kawakami, and H. Esaki, “A DTN-based sensor data gathering for agricultural applications,” *IEEE Sensors Journal*, vol. 11, no. 11, pp. 2861–2868, 2011.
- [30] D. Ehrlich, J. E. Estes, J. Scepan, and K. C. McGwire, “Crop area monitoring within an advanced agricultural information system,” *Geocarto International*, vol. 9, no. 4, pp. 31–42, 1994.
- [31] T.-Y. Lin, H. A. Santoso, K.-R. Wu, and G.-L. Wang, “Enhanced deployment algorithms for heterogeneous directional mobile sensors in a bounded monitoring area,” *IEEE Transactions on Mobile Computing*, vol. 16, no. 3, pp. 744–758, 2017.
- [32] A. Guerriero, F. Giuliani, and D. O. Nitti, “Crowdsourcing and mobile device for wide areas monitoring,” in *Proceedings of the 2015 IEEE Workshop on Environmental, Energy, and Structural Monitoring Systems (EESMS)*, pp. 29–32, Trento, Italy, July 2015.
- [33] C. Zygowski and A. Jaekel, “Path Planning for maximizing area coverage of mobile nodes in wireless sensor networks,” in *Proceedings of the 2018 IEEE 9th Annual Information Technology, Electronics and Mobile Communication Conference (IEMCON)*, pp. 12–17, Vancouver, BC, Canada, November 2018.
- [34] I. Khoufi, P. Minet, and N. Achir, “Unmanned aerial vehicles path planning for area monitoring,” in *Proceedings of the 2016 International Conference on Performance Evaluation and Modeling in Wired and Wireless Networks (PEMWN)*, pp. 1–5, Paris, France, November 2016.
- [35] Y. Chen and Y. Chen, “Path planning in large area monitoring by drones,” in *Proceedings of the 2018 Tenth International Conference on Advanced Computational Intelligence (ICACI)*, pp. 295–299, Xiamen, China, March 2018.



Hindawi

Submit your manuscripts at
www.hindawi.com

